Title

Simple yield surface expressions appropriate for soil plasticity

Journal

International Journal of Geomechanics, 10(4)

Authors

Taiebat, Mahdi
Dafalias, Yannis

Publication Date

2010-08-01

Simple Yield Surface Expressions Appropriate for Soil Plasticity

Mahdi Taiebat, A.M.ASCE[1]; and Yannis F. Dafalias, M.ASCE[2]

Abstract: The objective of this paper is to present a number of simple, practical, and useful analytical expressions of a yield surface for geomaterials. In classical plasticity, the analytical expression of a yield surface defines the locus of points in stress space at which plastic flow initiates, and the corresponding function must depend on direct and mixed invariants of stress and tensor-valued internal variables. One single function describes a yield surface in order to avoid singularities and computational difficulties arising from the use of multiple functions representing intersecting surfaces in stress space that are often used for cap-type models in soil plasticity. The presented functions are conveniently subdivided in three main categories depending on the type of analytical expression used, and they all describe properly closed yield surfaces which are continuous and convex. The internal variables in these functions can be used in order to address classical plasticity features such as isotropic and kinematic hardening, the latter in the form of rotational hardening. The effects of parameters on the shape of yield surfaces are clearly demonstrated and illustrated for all functions in triaxial stress space. The generalization of these functions to the multiaxial stress space is presented using a consistent method such that if one applies triaxial loading conditions on the multiaxial expressions, the triaxial ones are retrieved. Finally, the appropriateness of the yield functions in regards to the soil type is discussed.

DOI: 10.1061/(ASCE)GM.1943-5622.0000059

CE Database subject headings: Soil properties; Plasticity; Sand, soil type; Clays; Kinematics; Anisotropy.

Author keywords: Yield surface shape; Soil plasticity; Sand and clay; Kinematic hardening; Soil anisotropy.

Introduction

The purpose of this paper is to present a number of options for the analytical description of the shape of yield surface in stress space by a single function, which were found to be practical and useful for soil plasticity. The paper also analyzes some of the properties of these options, as well as the advantages and disadvantages vis-á-vis their use for various kinds of soils, in particular clays and sands. This is a narrower scope than the one in other works such as Desai (1980) and Desai et al. (1986) where a thorough examination of various analytical expressions in terms of direct and joint isotropic invariants of stress and other internal variables was conducted. In the present work, the focus is on specific choices of yield surfaces many of which have been already used to simulate experimental data, and some of which cannot be placed under the general framework of the aforementioned works and other similar ones. The idea is to actually present what, in the opinion of the writers, may be best suited for soil plasticity from a practical perspective, depending on the kind of soil and loading conditions, while maintaining as simple as possible the analytical description. Hence, the family of various surfaces examined here is more focused and restrictive than in other works, but had they been addressed in the past, due reference is given in the course of presentation.

The common characteristics of these yield surface options are:

1. They are closed surfaces and the size of each surface is controlled by an internal variable p_0 whose variation should be defined using an isotropic hardening rule.
2. Anisotropy of the material is represented by a stress ratio type of internal variable α, scalar-valued in triaxial, and tensor-valued in multiaxial stress space, whose variation is defined by an appropriate kinematic hardening rule inducing what is known as rotational hardening.

The analytical expressions of the yield surfaces are presented first in triaxial space, where they are discussed and illustrated, and then in multiaxial stress space by a consistent method of generalization from triaxial to multiaxial, such that if one applies triaxial loading conditions on the multiaxial expressions, the triaxial ones are retrieved. The analytical expressions of the yield surfaces are divided in three large groups of different analytical basis. For each group, various particular choices are presented and details of the corresponding yield surface features in stress space are discussed, which are useful for the expected soil response under different loading conditions. In the following, all stresses are considered effective. Illustrative plots are presented in the triaxial $p-q$ space.

It should be noted that modern ideas of thermodynamics, which are based on the fundamental physical concepts of work, energy, and dissipation, can be used for developing the elements of constitutive models. The yield loci, plastic potentials, flow rules, and isotropic and kinematic hardening rules can be deduced in a systematic manner from the free energy and dissipation po-

[1]Dept. of Civil Engineering, Univ. of British Columbia, Vancouver, BC, Canada V6T 1Z4 (corresponding author). E-mail: mtaiebat@civil.ubc.ca

[2]Dept. of Civil and Environmental Engineering, Univ. of California, Davis, CA 95616; and Dept. of Mechanics, National Technical Univ. of Athens, Zographou 15780, Hellas. E-mail: jfdafalias@ucdavis.edu

Note. This manuscript was submitted on December 5, 2008; approved on January 12, 2010; published online on January 15, 2010. Discussion period open until January 1, 2011; separate discussions must be submitted for individual papers. This paper is part of the ***International Journal of Geomechanics***, Vol. 10, No. 4, August 1, 2010. ©ASCE, ISSN 1532-3641/2010/4-161–169/$25.00.

tential functions. The introduction of a dissipation potential function is, in essence, a form of a constitutive assumption, which, together with the fundamental concept of free energy, create a much tighter analytical environment within which an elastoplastic model can rigorously be developed, guaranteed to satisfy the second law of thermodynamics. Such solid theoretical framework, however, often requires some compromise vis-á-vis experimental data for the evolution laws of the internal variables which enter the foregoing potentials. In particular for soils, such thermomechanical framework of elastoplasticity has been presented initially by Houlsby (1981, 1982) and Modaressi et al. (1994) followed by a more general and systematic approach in recent years by Collins and Houlsby (1997), Collins and Kelly (2002), Collins (2002), and Collins and Hilder (2002). The present paper, however, does not attempt to consider derivations from thermodynamics and has a more humble theoretical scope, namely, the presentation of a geometrical and analytical exposition of yield surface shapes which can bear serious consequences in the final stage of soil modeling. Many of the yield surface shapes to be presented have been found to fit experimentally determined yield points in stress space or stress-strain curves and stress paths, but no attempt will be made to repeat such data fitting since the main intention of the present work is to help the future researchers by systematizing the presentation of various yield surface expressions. Although it is common practice to introduce yield surface expressions based on experimental data for yielding of soils without reference to thermodynamics, it will be expedient to consider such questions in future exploitation of the yield surface shapes presented in conjunction with the rate equations for the involved internal variables, at least from the perspective of satisfying the second law of thermodynamics with or without the explicit introduction of a dissipation potential at the outset. The aforementioned works can provide a solid background and guidance for such an endeavor.

Analytical Expressions of Yield Surfaces in Triaxial Space

Elliptical Functions

The original equation for the elliptical plastic potential and yield surface (associative flow rule) of the modified Cam-clay model by Roscoe and Burland (1968) reads in the $p-q$ space as

$$f = q^2 - M^2 p p_0 \left(1 - \frac{p}{p_0}\right) = 0 \tag{1}$$

with M=critical state stress ratio and p_0=measure of equivalent isotropic preconsolidation effective pressure. This surface intersects the p axis at 0 and p_0 and the critical state stress ratio line (CSL) $\eta = q/p = M$ at a point where $\partial f/dp = 0$ (top point of the ellipse). The following two modifications of Eq. (1) are proposed along the lines described in the Introduction. First, the M is substituted by a factor N that may acquire a number of expressions not necessarily fixed, which control the shape of the yield surface. Second, in order to account for anisotropy manifested as a rotation of the yield surface and measured by a dimensionless stress ratio type internal variable α, one can substitute $q - p\alpha$ for q so that the yield surface Eq. (1) becomes

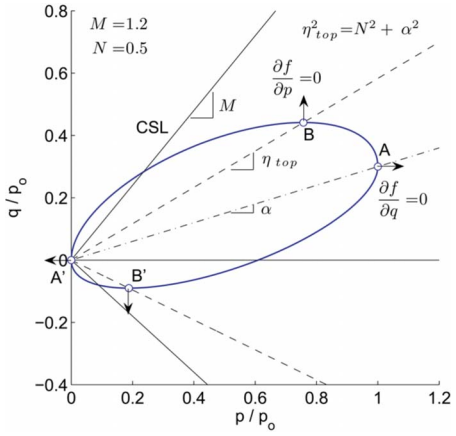

Fig. 1. Schematic illustration of the anisotropic elliptical yield surface in normalized $p-q$ space

$$f = (q - p\alpha)^2 - N^2 p p_0 \left(1 - \frac{p}{p_0}\right) = 0 \tag{2}$$

As shown in Fig. 1, Eq. (2) represents a sheared and rotated ellipse with the degree of rotation determined by the value of α. The normal to $f=0$ at different characteristic points is shown by a corresponding arrow. The normals to the surface at point A where $\eta = q/p = \alpha$, henceforth called the tip, and point A' which is the origin, are along the p-axis which means that at these points $\partial f/dq = 0$. Observe that p_0 is the p-coordinate of point A which is different from the value of p at the intersection of the surface with the p-axis; these two points coincide only when $\alpha = 0$. The normals at points B and B', the top and bottom points of the yield surface, are along the q-axis, hence, $\partial f/dp = 0$. These points are of interest in constitutive modeling of clays in critical state soil mechanics (CSSM), in particular if the yield surface is to be considered also the plastic potential surface for associative flow rule plasticity. In such a case, the normal to the plastic potential at the critical state $\eta = M$ should have zero component along the p-axis which implies the critical state condition of zero volumetric plastic strain rate. Therefore, the rotational hardening rule of such model which defines the evolution of α should guarantee that upon shearing the current stress point eventually finds itself at points B or B' reaching simultaneously the CSL which is shown as usual with slope M in Fig. 1 and all figures thereafter. To this extend it becomes important to identify in all subsequent choices the top (and bottom) stress ratio η_{top} by setting $\partial f/dp = 0$ (which corresponds to points A or A') in Eq. (2) and solving for $\eta = \eta_{top}$ to obtain the general expression

$$\eta^2_{top} = N^2 + \alpha^2 \tag{3}$$

Eq. (3) provides the guidelines for subsequent choices of N in the sense of defining the corresponding η_{top}. The following four of such choices are presented here.

Choice 1

The first choice that comes in mind, motivated by the original Cam-clay Eq. (1), is to set

$$N^2 = M^2 \Rightarrow \eta^2_{top} = M^2 + \alpha^2 \tag{4}$$

where use of Eq. (3) was made. Eq. (4) indicates that at the top point where $\partial f/dp = 0$ the $\eta_{top} \geqslant M$, the equality holding when $\alpha = 0$. For that reason this is an acceptable choice if one establishes experimentally that there is a change of the critical stress

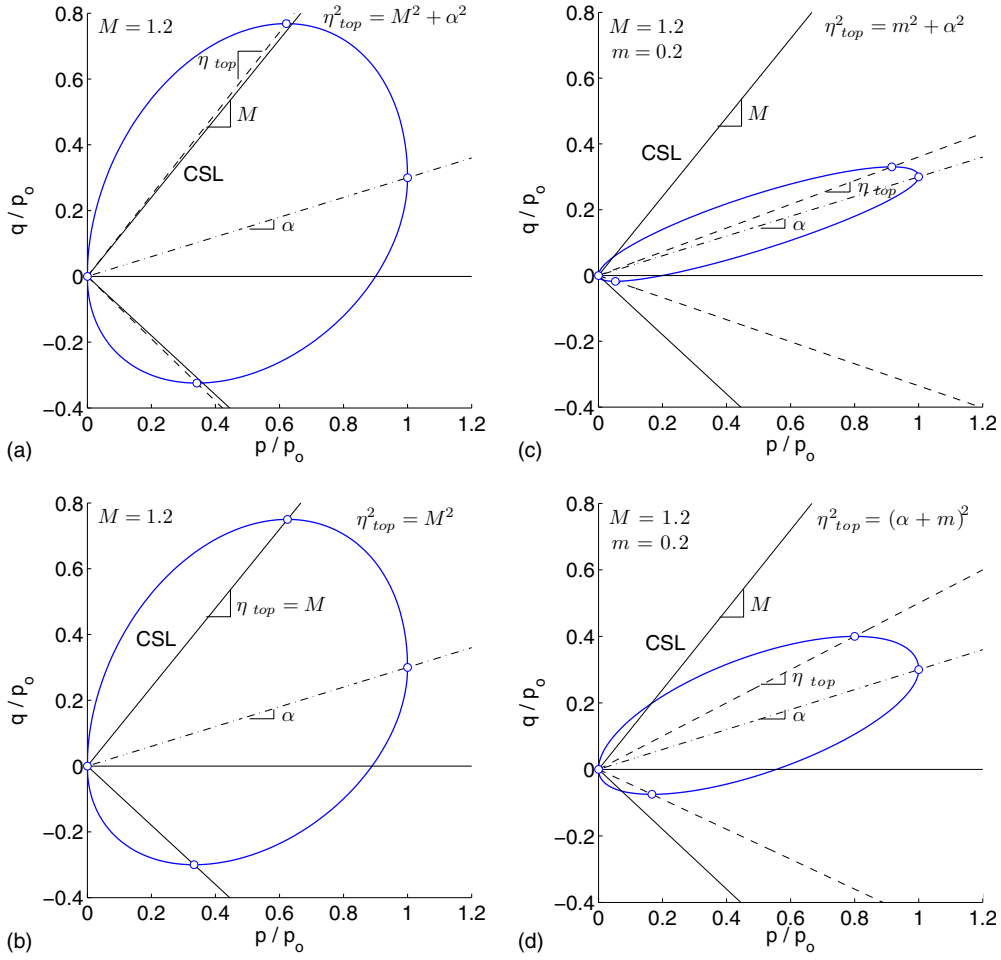

Fig. 2. Schematic illustration of four different choices for the factor N in the anisotropic elliptic yield surface: (a) Choice 1: $N^2=M^2$; (b) Choice 2: $N^2=M^2-\alpha^2$; (c) Choice 3: $N^2=m^2$; and (d) Choice 4: $N^2=(\alpha+m)^2-\alpha^2$; the stress-ratio quantity m is a measure of the difference between η_{top} and α in (c) and (d)

ratio, measured by η_{top}, from M to something larger due to anisotropy measured by α. Such increase is not often observed, and if there is some, it is very small. In that case the present option may work well because, as it is illustrated in Fig. 2(a), the change from M to η_{top} is very mild for a reasonable value of rotation due to α; for larger values of α, this difference increases, yet within limits. The relatively small effect the α has on η_{top} in relation to M is due to the second power relation among η_{top}, M, and α. The difference in *shape* of the half top and bottom of the yield surface is because different values of M were used on the compression and extension sides.

Choice 2

Aiming at maintaining $\eta_{top}=M$ for any value of anisotropy measured by α due to the aforementioned reasons required by CSSM, Eq. (3) suggests the choice

$$N^2 = M^2 - \alpha^2 \Rightarrow \eta_{top}^2 = M^2 \tag{5}$$

This option is what Dafalias (1986) proposed from a nongeometrical perspective, based on the simplest possible extension of the energy assumption of the modified Cam-clay model which leads from isotropic to anisotropic response. The surface was obtained from integration of a rate of plastic work equation in triaxial $p-q$ space in which coupling between the plastic deviatoric and volumetric strain rates was introduced via α. The resulting plastic potential surface, which for associative plasticity serves also as a yield surface, was verified experimentally and used by various writers in constitutive modeling of clays (Dafalias 1987; Korhonen and Lojander 1987; Thevanayagam and Chameau 1992; Newson and Davies 1996; Wheeler et al. 1999, 2003). For the required positive sign of the term $M^2-\alpha^2$ this choice of N demands that $|\alpha|<M$. Fig. 2(b) illustrates the shape of the yield surface for a reasonable value of α. The top (and bottom) points of the rotated and sheared ellipse always intersect the $\eta=M$ lines for any value of α. Again, observe the difference in shape of the half top and bottom of the yield surface due to different values of M on the compression and extension sides, as in Choice 1.

Choice 3

As can be seen from Fig. 2(a) or Fig. 2(b), the resulting yield surface shape is quite *bulky*, encompassing a large elastic range. This is because, in both cases, the η_{top} is related to M which is in general large. It is often desired, though, to have a yield surface which is rather slender with a small dimension along the q axis, as, for example, it would have been the case if one chose a small value for M. Since M is fixed by the soil properties, an alternative way would be to introduce a new parameter m by making the choice

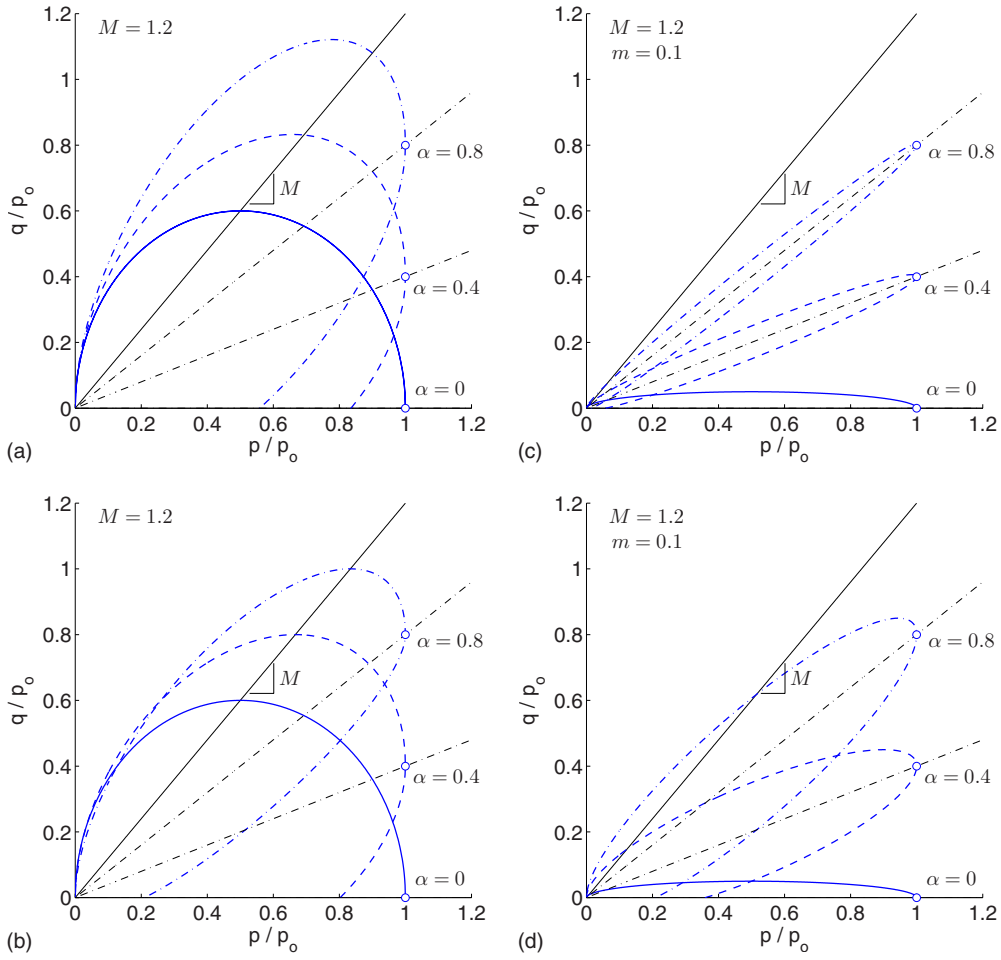

Fig. 3. Effect of the backstress ratio α on the shapes of the elliptical yield surface for all four different choices for the factor N: (a) Choice 1: $N^2=M^2$; (b) Choice 2: $N^2=M^2-\alpha^2$; (c) Choice 3: $N^2=m^2$; and (d) Choice 4: $N^2=(\alpha+m)^2-\alpha^2$

$$N^2 = m^2 \Rightarrow \eta_{\text{top}}^2 = m^2 + \alpha^2 \tag{6}$$

where $m << M$. The parameter m provides freedom in choosing the slenderness of the yield surface as it is illustrated in Fig. 2(c). Such choice requires the definition of a prudent evolution law for the internal variable α so that the value of η_{top} does not exceed M for associative flow rule plasticity. The resulting yield surface for this choice of N was in fact proposed in the MIT-E3 model (Whittle and Kavvadas 1994) to describe the generalized behavior of K_0-normally consolidated clays, based on earlier works of Kavvadas (Kavvadas 1982).

Choice 4

Along the same line of searching for a slender yield surface, a more intuitive and direct relation between the parameter m and the values of M and α is obtained by the choice

$$N^2 = (|\alpha| + m)^2 - \alpha^2 \Rightarrow \eta_{\text{top}}^2 = (|\alpha| + m)^2 \tag{7}$$

where the absolute value of α is introduced because the α can acquire positive and negative values. Again, one must be careful when evolution laws for α are postulated so that the $M-m$ is the limit of $|\alpha|$ in order to keep $\eta_{\text{top}} \leq M$. Fig. 2(d) illustrates this type of yield surface.

In the illustrations of the first and second choices in Figs. 2(a and b), the values $M_c=1.2$ and $M_e=0.75M_c=0.9$ are used to distinguish between the compression ($\eta > \alpha$) and extension ($\eta < \alpha$) values of parameter M. For the third and fourth choices in Figs. 2(c and d) the value of $m_c=m_e=0.2$ is used. The parameter m here is left the same in compression and extension but one can control the evolution of α so that η_{top} does not exceed the M_c or M_e, i.e., different bounds in compression and extension for α.

An important attribute of the yield surface shape one must account for is how it changes with various degrees of anisotropy measured in ascending order by an increasing value of $|\alpha|$. An illustration of this change is shown in the four parts of Fig. 3 for the foregoing four choices and for three values of $|\alpha|=0$, 0.45, and 0.8, with M_c, M_e, m_c, and m_e, as in Fig. 2. Observe that for the first choice in Fig. 3(a) the value of η_{top} is clearly different from that of M_c for $\alpha=0.8$, while for the first two values of α, η_{top} is almost equal to M_c. For the second choice shown in Fig. 3(b) $\eta_{\text{top}}=M_c$ for all values of α, as expected, but observe for $\alpha=0.8$ the strong *flattening* of the bottom part of the yield surface drawn below the line of α, which is calculated based on $M_e=0.75M_c=0.9$ and the corresponding Eq. (2); this is because as α approaches the value of $M_e=0.9$ the corresponding equation for the bottom part of the yield surface (the triaxial extension part) degenerates to that of a straight line with slope α. The same thing would happen for the top part of the yield surface as α approaches M_c, but by this time, there is no real-valued expression for the bottom part since $\alpha \geq M_e$. Hence, the evolution law must not allow α to grow above the smallest of M_c and M_e, that being usually M_e. In Fig. 3(c) observe that the initial slenderness of the rotated ellipse, measured by m, remains almost the same for all

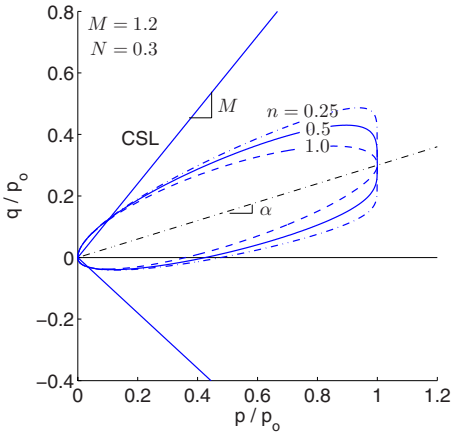

Fig. 4. Effect of the power n on p/p_0 term of the elliptical function

values of α, while in Fig. 3(d) the corresponding slenderness measured again by m appears to reduce for larger values of α.

In all of the above choices, one can control the relative sharpness of the elliptical yield surface at the origin and at the tip (i.e., at $p=p_0$) by a power of the p/p_0 term. A power of n, such that $n \leqslant 1$, can be used to modify the generic Eq. (2) as

$$f = (q - p\alpha)^2 - N^2 p p_0 \left[1 - \left(\frac{p}{p_0} \right)^n \right] = 0 \tag{8}$$

The effect of raising p/p_0 to the power n is illustrated in Fig. 4 for different values of $n=1$, 0.5, and 0.25 in an anisotropic elliptical yield surface with $\alpha=0.3$ and $N=0.3$. It can be observed that smaller values of n cause a wider opening at the tip of the yield surface at $p=p_0$, almost like a flat cup. This may prove useful for cases that a closed yield surface with thinner shape at the origin and thicker shape at the tip is needed due to pressure sensitivity, etc., and may be appropriate for rock material type.

Lemniscate

Modified Lemniscate of Bernoulli

The original equation of the *Lemniscate of Bernoulli,* also termed the *hyperbolic lemniscate,* in the Cartesian coordinate system is (Lawrence 1972)

$$(p^2 + q^2)^2 = p_0^2 (p^2 - q^2) \tag{9}$$

By substituting q with $(q-p\alpha)/m$, one can control the shape and orientation of this surface. With this substitution the equation can be reduced to the following form:

$$f = (q - p\alpha)^2 - m^2 p^2 \left[1 - \left(\frac{p}{p_0} \right)^2 \gamma^2 \right] = 0 \tag{10a}$$

$$\gamma = 1 + \left(\frac{q - p\alpha}{mp} \right)^2 \tag{10b}$$

where the factor m controls the slenderness of the shape. Fig. 5(a) illustrates the effect of the parameter m while Fig. 5(b) that of an increasing α. One can compute the value of η_{top} which depends on α by solving the equation $\partial f/\partial p=0$ for η. Hence, restrictions on the maximum value of $|\alpha|$ must be imposed so that $\eta_{top} \leqslant M$. A basic difference of the modified lemniscate from the elliptical shapes is that at the origin it forms a sharp corner measuring the

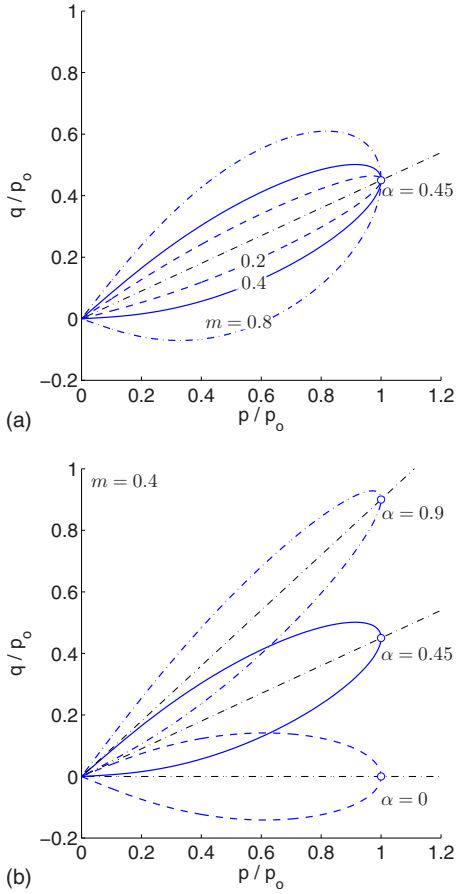

Fig. 5. Schematic illustration of the anisotropic yield surface using the lemniscate of Bernoulli function and the effects of the parameter m and the backstress ratio α on the shapes of the resulting yield surfaced

opening of the lemniscate, while for the elliptical choices of Eq. (2), the shape is smooth with a tangent line parallel to the q axis at the origin. Notice from Fig. 5(b) that as α increases this sharp corner at the origin rotates with the lemniscate.

Distorted Lemniscate

Pestana and Whittle (1999) have introduce the following form for the yield surface of a unified model for sand and clay

$$f = (q - p\alpha)^2 - \zeta^2 p^2 \left[1 - \left(\frac{p}{p_0} \right)^n \right] = 0 \tag{11a}$$

$$\zeta^2 = m^2 + \alpha^2 - 2\frac{q}{p}\alpha \tag{11b}$$

As shown in the three parts of Fig. 6, where also the effect of the parameters m, n and the variable α is shown, the shape of the yield surface resembles a distorted lemniscate, hence, the name the writers attributed to their yield surface. This yield surface also forms a sharp corner at the origin but unlike the lemniscate of the previous case, this sharp corner does not rotate as the value of α increases with consequences to be commented upon in the sequel. Also, it follows that, in order to maintain the positive sign of the right-hand side of Eq. (11*b*), α must not exceed the value of m; in fact, as α approaches m, the top part of the distorted lemniscate

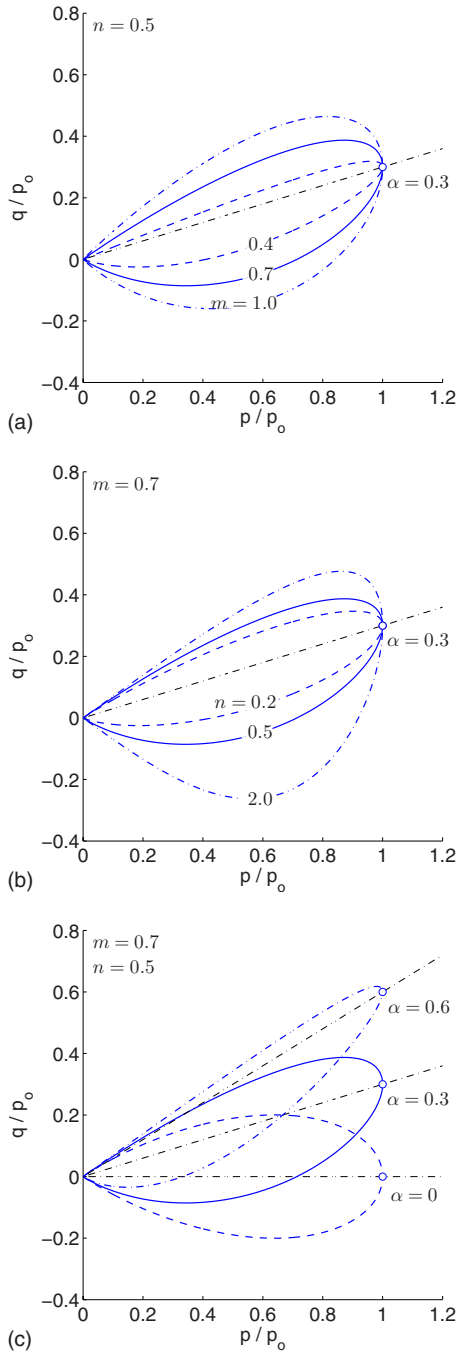

Fig. 6. Schematic illustration of the anisotropic yield surface using the distorted lemniscate of Bernoulli function and the effects of the parameters m and n and the backstress ratio α on the shapes of the resulting yield surfaced

tends to degenerate into a straight line of slope m, as shown in Fig. 6(c) when $\alpha=0.6$ for the choice $m=0.7$.

Eight-Curve

The motivation for the last family of yield surfaces came from the work of Manzari and Dafalias (1997) where a thin open wedge with its tip at the origin was chosen as the yield surface for sands, based on the predominance of the stress ratio variation as the main cause of plastic deformation in sand. The wedge could rotate around the origin in the familiar form of rotational hardening (as the previous yield surfaces do) but it was open toward increasing values of p, thus, not being able to induce plastic deformations under loading at constant stress ratio. Nevertheless the very thin wedge shape offered many advantages for the description of the sand response under cyclic loading, thus, it was desirable to preserve it and simultaneously find a way to close the wedge by a single analytical expression without introducing a separate closing cup equation as often done in other works for the so-called cap models. It proved to be easier than initially thought. The basis was the so-called original eight-curve, because it resembles the number eight if plotted in Cartesian coordinates according to the analytical expression (Lawrence 1972)

$$p^4 = p_0^2(p^2 - q^2) \tag{12}$$

Again, the above expression must be modified in order to be useful as a yield surface. To this extent, rotational hardening is introduced as previously by the substitution of $(q-p\alpha)/m$ for q in Eq. (12), where the additional factor m is introduced to control the opening at the origin. In addition, the curvature of the cup-type closure can be controlled by raising the p/p_0 to the power of $n \geqslant 2$. With these modifications, the analytical expression of the original eight-curve becomes the yield surface equation

$$f = (q - p\alpha)^2 - m^2p^2\left[1 - \left(\frac{p}{p_0}\right)^n\right] = 0 \tag{13}$$

The effect of the parameters m, n, and the variable α is shown in the three parts of Fig. 7. In all cases, the yield surface becomes exactly a wedge in the limit as the origin is approached, and maintains the wedge-type form for most of its *length* along increasing p, in particular for the higher values of the parameter n. For such higher values of n, the closing cup-type shape acquired by the yield surface as p approaches p_0 resembles more a straight line cup, but recall that it is one single analytical description that gives all these features. Also observe that the wedge at the origin rotates together with α, as opposed to what happens for the distorted lemniscate whose wedge shape at the origin remains unchanged as α increases. It is also interesting to compare the form of Eq. (13) with that of Eq. (4) for the modified elliptical shapes. In Eq. (4), the term N^2pp_0 is substituted by the term m^2p^2 of Eq. (13), and with the choice $N=m$ it follows that the only difference is that a p_0 appears in Eq. (4) instead of p in Eq. (13), yet, this difference can create the different shapes of Figs. 4 and 7. Had the numerical value of N of Fig. 4 been chosen smaller, the yield surfaces would have been of equal slenderness as those of Fig. 7, but no wedge-type shape would appear at the origin where still the tangent would be parallel to the q axis. The yield surface given by Eq. (13) was introduced in the recent SANISAND model by Taiebat and Dafalias (2008). It also requires careful control of the absolutely maximum value of α so that critical failure occurs at $\eta=M$.

Multiaxial Generalization

There is a systematic approach to generalize the yield surface equations presented so far from the triaxial to multiaxial setting, such that when triaxial loading conditions are imposed on the multiaxial expressions, they become identical to their triaxial counterparts characterized by the same parameters (or model constants) in both spaces. Henceforth, all second order tensors will be denoted by bold face. The stress tensor is denoted by $\boldsymbol{\sigma}$. The

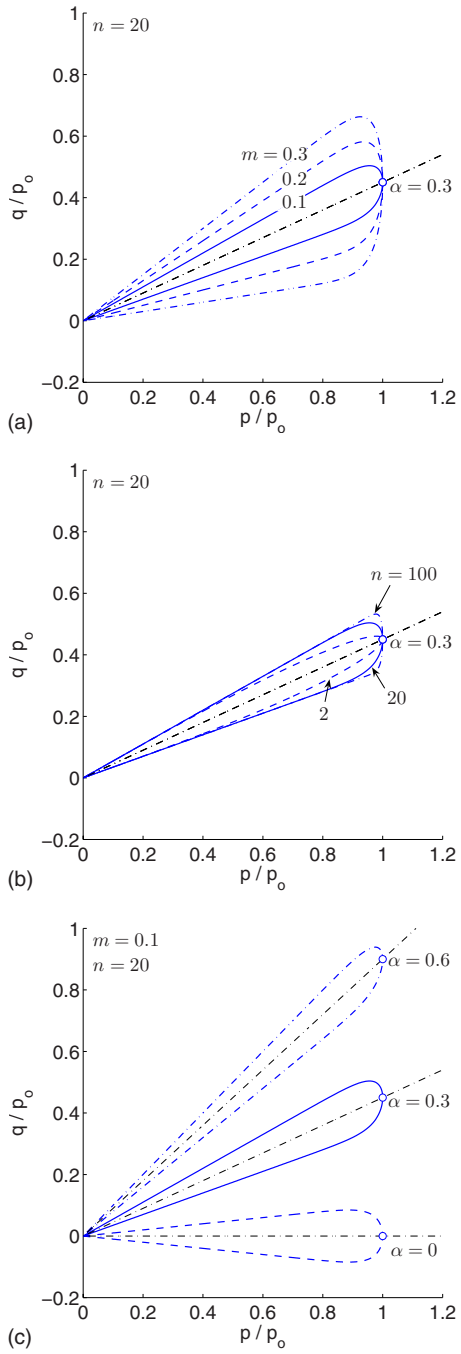

Fig. 7. Schematic illustration of the anisotropic yield surface using the eight-curve function and the effects of the parameters m and n and the backstress ratio α on the shapes of the resulting yield surfaced

hydrostatic or isotropic stress p and the deviatoric or shear stress tensor $\mathbf{s}$ are defined by $p=(\text{tr}\ \boldsymbol{\sigma})/3$ and $\mathbf{s}=\boldsymbol{\sigma}-p\mathbf{I}$, where tr means the trace, and $\mathbf{I}$ is the identity tensor.

The multiaxial generalization of the yield surface expressions is based on the following observation. In a triaxial setting any deviatoric symmetric tensor $\mathbf{t}$ develops only normal components t_i $(i=1,2,3)$ with $\text{tr}\ \mathbf{t}=0$, which means $t_2=t_3=(-1/2)t_1$. It is straightforward to show that the following relation holds true

$$\frac{3}{2}\mathbf{t}:\mathbf{t}=(t_1-t_3)^2 \tag{14}$$

where the symbol : implies the trace of the product of two adjacent tensors, which is $\mathbf{t}:\mathbf{t}=\text{tr}\ \mathbf{t}^2$. This is a general equation which constitutes the basis of the current systematic multiaxial generalization. For instance, substituting the deviatoric stress tensor $\mathbf{s}$ into Eq. (14), one has $(3/2)\mathbf{s}:\mathbf{s}=(s_1-s_3)^2$, and knowing that $(s_1-s_3)=(\sigma_1-\sigma_3)=q$, the following relation between the deviatoric stress tensor $\mathbf{s}$ and its triaxial counterpart q can be observed when triaxial conditions are assumed

$$\frac{3}{2}\mathbf{s}:\mathbf{s}=q^2 \tag{15}$$

Along the lines of this equation, one can introduce the deviatoric stress-ratio tensor $\mathbf{r}=\mathbf{s}/p$, the deviatoric backstress ratio tensor $\boldsymbol{\alpha}$, and the effective deviatoric stress tensor $\mathbf{s}-p\boldsymbol{\alpha}$, as the multiaxial counterparts of the triaxial entities η, α, and $q-p\alpha$, respectively, such that under triaxial conditions

$$\frac{3}{2}\boldsymbol{\alpha}:\boldsymbol{\alpha}=\alpha^2;\ \ \frac{3}{2}(\mathbf{s}-p\boldsymbol{\alpha}):(\mathbf{s}-p\boldsymbol{\alpha})=(q-p\alpha)^2;\ \ \frac{3}{2}\mathbf{r}:\mathbf{r}=\eta^2 \tag{16}$$

Notice that Eq. (16) implies that $\alpha=\alpha_1-\alpha_3$, with $\alpha_2=\alpha_3$ and with the observation that under triaxial conditions the tensor $\boldsymbol{\alpha}$ develops only normal components α_i $(i=1,2,3)$. This equivalence between multiaxial and triaxial stress spaces allows the geometrical interpretation of tensor-valued entities in the triaxial space where tensor components can be related to scalar-valued equivalent quantities.

Elliptical functions

Based on Eqs. (15) and (16), the analytical expression (2) of the elliptical surface generalizes to

$$f=\frac{3}{2}(\mathbf{s}-p\boldsymbol{\alpha}):(\mathbf{s}-p\boldsymbol{\alpha})-N^2pp_0\left(1-\frac{p}{p_0}\right)=0 \tag{17}$$

where the generalized forms of N^2 for the four corresponding cases, i.e., Eqs. (3)–(6), are

$$N^2=M^2 \tag{18a}$$

$$N^2=M^2-\frac{3}{2}\boldsymbol{\alpha}:\boldsymbol{\alpha} \tag{18b}$$

$$N^2=m^2 \tag{18c}$$

$$N^2=\left(\sqrt{\frac{3}{2}\boldsymbol{\alpha}:\boldsymbol{\alpha}}+m\right)^2-\frac{3}{2}\boldsymbol{\alpha}:\boldsymbol{\alpha} \tag{18d}$$

respectively. The critical stress ratio M in Eqs. (18*a*) and (18*b*) requires different values of M_c and M_e according to the sign of $(\eta-\alpha)$ as explained after Eq. (7). In the multiaxial stress space the M will be interpolated between its values M_c and M_e by means of lode angle θ, according to the proposition by Argyris et al. (1974), which with $c_M=M_e/M_c$ reads as

$$M=\Theta(\theta,c_M)M_c=\frac{2c_M}{(1+c_M)-(1-c_M)\cos 3\theta}M_c \tag{19}$$

$$\cos 3\theta=\sqrt{6}\text{tr}\ \mathbf{n}^3;\ \ \mathbf{n}=\frac{\mathbf{r}-\boldsymbol{\alpha}}{[(\mathbf{r}-\boldsymbol{\alpha}):(\mathbf{r}-\boldsymbol{\alpha})]^{1/2}} \tag{20}$$

The relations $\text{tr}\ \mathbf{n}=0$ and $\text{tr}\ \mathbf{n}^2=\mathbf{n}:\mathbf{n}=1$ hold true. The values $\theta=0$ and $\theta=\pi/3$ correspond to effective stress ratio definition of

compression and extension, respectively, where the effective stress ratio $\mathbf{r}-\boldsymbol{\alpha}$ (equivalent to $\eta-\alpha$) rather than the stress ratio $\mathbf{r}$ is used to define $\mathbf{n}$ and subsequently θ. The parameter m can be left the same in compression and extension, as it was explained before, with no interpolation in the multiaxial stress space. Of course, if different values of this parameter in compression and extension are needed one can apply a similar generalization rule to the one already presented for M.

Finally the scalar term $(p/p_0)^n$ in Eq. (8) remains unchanged in the multiaxial generalization.

Lemniscate

The generalization of Eqs. (10*a*) and (10*b*) for the modified lemniscate of Bernoulli and Eqs. (11*a*) and (11*b*) for the distorted lemniscate follow the same rule. For the modified lemniscate of Bernoulli, the generalized form of the equations are

$$f = \frac{3}{2}(\mathbf{s}-p\boldsymbol{\alpha}):(\mathbf{s}-p\boldsymbol{\alpha}) - m^2p^2\left[1-\left(\frac{p}{p_0}\right)^2\gamma^2\right] = 0 \quad (21a)$$

$$\gamma = 1 + \frac{3}{2}(\mathbf{s}-p\boldsymbol{\alpha}):(\mathbf{s}-p\boldsymbol{\alpha})\left(\frac{1}{mp}\right)^2 \quad (21b)$$

and for the distorted lemniscate

$$f = \frac{3}{2}(\mathbf{s}-p\boldsymbol{\alpha}):(\mathbf{s}-p\boldsymbol{\alpha}) - \zeta^2p^2\left[1-\left(\frac{p}{p_0}\right)^n\right] = 0 \quad (22a)$$

$$\zeta^2 = m^2 + \frac{3}{2}\boldsymbol{\alpha}:\boldsymbol{\alpha} - 2\sqrt{\left(\frac{3}{2}\mathbf{r}:\mathbf{r}\right)\left(\frac{3}{2}\boldsymbol{\alpha}:\boldsymbol{\alpha}\right)} \quad (22b)$$

Again, here it may be enough to use the same values for parameter m in compression and extension but generalization is straightforward if needed.

Eight-Curve

Finally the generalized form of Eq. (13) for the eight-curve function reads

$$f = \frac{3}{2}(\mathbf{s}-p\boldsymbol{\alpha}):(\mathbf{s}-p\boldsymbol{\alpha}) - m^2p^2\left[1-\left(\frac{p}{p_0}\right)^n\right] = 0 \quad (23)$$

Discussion: Sand or Clay?

Having presented a number of yield surface shapes it is natural to discuss their appropriateness in regards to soil type. Here, a restriction to two basic types of soils will be considered, that of sands and clays. The most characteristic difference between sands and clays from the perspective of plastic constitutive modeling is the loading direction which is normal to the yield surface. In sands, due to their granular nature, the predominant mechanism of plastic deformation is due to a change in stress ratio, while in clays loading under constant stress ratio produces large plastic deformations, as, for example, under K_0 conditions. An additional difference is that for sands the purely elastic range enclosed by a yield surface appears to be much smaller than that for a clay, although in principle, one can argue that in general a pure elastic range for soils is almost nonexisting.

Therefore, within the modeling possibilities of plasticity, a yield surface for clays must be a closed surface producing plastic deformation early in a loading process under a constant stress ratio while the yield surface for sands must be narrow with a shape that is more or less along a constant stress ratio line in the triaxial space, and for higher values of p such shape must be closed, since high pressure can create plastic deformation by crushing of the sand grains. Among the previously presented shapes, Choices 1 and 2 of the elliptical shapes as well as the distorted lemniscate are appropriate for clays, while Choices 3 and 4 of the elliptical shapes involving the slenderness parameter m, the two lemniscates, and the eight-curve appear to fulfill the aforementioned requirements for a yield surface for sands, as long as the value of m is sufficiently small. However, a problem may arise for the distorted lemniscate elaborated in the following.

While the foregoing appear to be only qualitative assessments, there is an interesting thought experiment which can delineate the appropriateness of a yield surface for sands or clays. This is related to possible change of stress within the yield surface or tangentially to it in what is known a neutral loading path, which can lead to experimentally unacceptable results. For example, consider the intersection of the yield surface with the p axis, and starting from this intersection point, follow a loading path within or tangentially to the yield surface toward increasing stress ratios in the triaxial space. If the shape of the yield surface is such as to allow high values of stress ratio to be reached from the zero initial value on the p axis, then such yield surface is not appropriate for sands because it implies that one can increase the stress ratio without inducing any plastic deformation contrary to experimental data which show a great sensitivity of sand plastic deformation to stress ratio changes, largely independent of the confining pressure. Clearly, and for reason exposed before, the aforementioned Choices 1 and 2 of the elliptical shape are not appropriate for sands. In regards to the remaining shapes, let us compare the choice 3 of the elliptical shape shown in Fig. 3(c) and the distorted lemniscate shown in Fig. 6(c) for various values of α, in particular for higher values of it and a small value of m controlling their slenderness. Both surfaces intersect the p axis for all α. This is not so clear in Fig. 3(c) due to the slenderness of the ellipse, but it clearly follows form the analytical description. Such intersection is clear for the distorted lemniscate as a result of the nonrotating with α opening wedge at the origin which guarantees an intersection with the p axis. Thus, one can perform the neutral loading test. In the case of Fig. 3(c), such test will follow a more or less fixed stress ratio path (the lower part of the rotated slender ellipse) justifying why no plastic deformation occurs, but in the case of Fig. 6(c) the neutral loading path can increase dramatically the value of the stress ratio given the "bulky" shape of the distorted lemniscate and its inescapable intersection with the p axis. Hence, the shape in Fig. 3(c) passes the neutral loading test while the shape in Fig. 6(c) does not, in order to be considered appropriate yield surface shapes for sand plasticity. Nevertheless, shapes which do not past the aforementioned test are used as yield surfaces for sands, often with success for the loading conditions considered, but there will always be lingering in the failure to predict correctly the sand response under neutral loading. The eight-curve modification of Fig. 7, which is clearly of a rotating wedge-type at the origin, passes the neutral loading test easily (in fact it was constructed to do so). In particular for values of α not very close to zero, the corresponding yield surface does not intersect the p axis due to the wedge rotation (unlike the distorted lemniscate's not rotating wedge), except at exactly the origin at zero effective stress. Its shape and position does not allow any

significant stress ratio change to occur during neutral loading, with the maximum change controlled by the slenderness parameter m which is chosen very small and reflects the stress ratio change occurring when one crosses the *width* of the wedge.

References

Argyris, J. H., Faust, G., Szimmat, J., Warnke, E. P., and Willam, K. J. (1974). "Recent developments in the finite element analysis of prestressed concrete reactor vessels." *Nucl. Eng. Des.*, 28(1), 42–75.

Collins, I. F. (2002). "Associated and non-associated aspects of the constitutive laws for coupled elastic/plastic materials." *Int. J. Geomech.*, 2(2), 259–267.

Collins, I. F., and Hilder, T. (2002). "A theoretical framework for constructing elastic/plastic constitutive models of triaxial tests." *Int. J. Numer. Analyt. Meth. Geomech.*, 26(13), 1313–1347.

Collins, I. F., and Houlsby, G. T. (1997). "Application of thermomechanical principles to the modelling of geotechnical materials." *Proc. R. Soc. London, Ser. A*, 453, 1975–2001.

Collins, I. F., and Kelly, P. A. (2002). "A thermomechanical analysis of a family of soil models." *Geotechnique*, 52(7), 507–518.

Dafalias, Y. F. (1986). "An anisotropic critical state soil plasticity model." *Mech. Res. Commun.*, 13(6), 341–347.

Dafalias, Y. F. (1987). "An anisotropic critical state clay plasticity model." *Proc., 2nd Int. Conf. on Constitutive Laws for Engineering Materials*, C. S. Desai, E. Krempl, P. Kiousis, and T. Kundu, eds., Vol. I, Elsevier Science, New York, 513–521.

Desai, C. S. (1980). "A general basis for yield, failure and potential functions in plasticity." *Int. J. Numer. Analyt. Meth. Geomech.*, 4(4), 361–375.

Desai, C. S., Somasundaram, S., and Frantziskonis, G. (1986). "A hierarchical approach for constitutive modelling of geologic materials." *Int. J. Numer. Analyt. Meth. Geomech.*, 10(3), 225–257.

Houlsby, G. T. (1981). "A study of plasticity theories and their application to soils." Ph.D. thesis, Univ. of Cambridge, Cambridge, U.K.

Houlsby, G. T. (1982). "A derivation of the small-strain incremental theory of plasticity from thermodynamics." *Proc., IUTAM Conf. on Deformation and Failure of Granular Materials*, Taylor and Francis, Delft, The Netherlands, 109–118.

Kavvadas, M. J. (1982). "Non-linear consolidation around driven piles in clays." Sc.D. thesis, Dept. of Civil and Environmental Engineering, Massachusetts Institute of Technology, Cambridge, Mass.

Korhonen, K. H., and Lojander, M. (1987). "Yielding of perno clay." *Constitutive Laws for Engineering materials: Theory and Applications, Proc., 2nd IC*, C. S. Desai, et al., eds., Vol. II, Elsevier Science, New York, 1249–1255.

Lawrence, J. D. (1972). *A catalog of special plane curves*, Dover, New York.

Manzari, M. T., and Dafalias, Y. F. (1997). "A critical state two-surface plasticity model for sands." *Geotechnique*, 47(2), 255–272.

Modaressi, H., Laloui, L., and Aubry, D. (1994). "Thermodynamical approach for Camclay-family models with Roscoe-type dilatancy rules." *Int. J. Numer. Analyt. Meth. Geomech.*, 18, 133–138.

Newson, T. A., and Davies, M. C. R. (1996). "A rotational hardening constitutive model for anisotropically consolidated clay." *Soils Found.*, 36(3), 13–20.

Pestana, J. M., and Whittle, A. J. (1999). "Formulation of a unified constitutive model for clays and sands." *Int. J. Numer. Analyt. Meth. Geomech.*, 23(12), 1215–1243.

Roscoe, K. H., and Burland, J. B. (1968). "On the generalized stress-strain behaviour of wet clay." *Engineering plasticity*, Cambridge University Press, Cambridge, U.K., 553–609.

Taiebat, M., and Dafalias, Y. F. (2008). "SANISAND: simple anisotropic sand plasticity model." *Int. J. Numer. Analyt. Meth. Geomech.*, 32(8), 915–948.

Thevanayagam, S., and Chameau, J. L. (1992). "Modelling anisotropy of clays at critical state." *J. Eng. Mech.*, 118(4), 786–806.

Wheeler, S. J., Karstunen, M., and Näätänen, A. (1999). "Anisotropic hardening model for normally consolidated soft clays." *Numerical Models in Geomechanics, Proc., NUMOG VII*, G. N. Pande, S. Pietruszczak, and H. F. Schweiger, eds., Vol. II, Balkema, Rotterdam, The Netherlands, 33–40.

Wheeler, S. J., Näätänen, A., Karstunen, M., and Lojander, M. (2003). "An anisotropic elastoplastic model for soft clays." *Can. Geotech. J.*, 40, 403–418.

Whittle, A. J., and Kavvadas, M. J. (1994). "Formulation of MIT-E3 constitutive model for overconsolidated clays." *J. Geotech. Eng.*, 120(1), 173–198.